JMEPEG (2007) 16:784–791
DOI: 10.1007/s11665-007-9097-0

1059-9495/$19.00

The Correlation of Machinability and Microstrutural Characteristics of Different Extruded Aluminum Alloys

André R. Froehlich, Ricardo Callegari Jacques, Telmo R. Strohaecker, and Ricardo Mombru

(Submitted July 7, 2005; in revised form October 18, 2006)

This work correlates metallurgical characteristics (chemical composition, microstructure and morphology of second phase particles) of different extruded aluminum alloys with their machinability as determined by the measurement of axial forces and shear momentum involved in drilling operations. Three different aluminum alloys were evaluated. The alloy AA6061 with low and high P content was tested in the recrystallized condition while alloys AA6351 and AA2117 were tested in the cold-worked condition. Specimen characterization also included tensile and hardness tests, chemical and microstructural evaluation. The results have shown that Pb and Cu have a positive effect on the machinability of these alloys and that the microstructure control may decrease forces in machining, resulting in great improvement of production in cutting procedures.

Keywords aluminum, machining, material selection

1. Introduction

The use of aluminum alloys in the industry is increasing in general because of its interesting technological characteristics, such as: low density, good-mechanical resistance, ductility, high toughness and good-corrosion resistance. Among the different fabrication processes the machining stage has a significant importance considering fabrication costs and processing time. Therefore, optimization of the process parameters that affect machining stages such as, tool wear, alloy machinability, machining efforts and cutting speed becomes an area of constant development and study.

Considering machinability as a characteristic of a given alloy, there are studies in the literature reporting the effects of metallurgical characteristics of the alloys as an important factor in their machinability.

In the view of chemical composition, Pb (Ref 1) and Bi additions are used to improve machinability in aluminum alloys, acting as lubricant and chip breakers (Ref 2, 3). The presence of Cu leads to the formation of $CuAl_2$ particles, which when refined and disperse, favors machinability by a decrease in plasticity, (Ref 4) and results in chip embrittlement (Ref 5). Additions of up to 1% Sn increase machinability in Al-Cu, Al-Cu-Si, and Al-Zn alloys (Ref 3). Besides that, Ti combined with B forms TiB_2 that acts as a grain refiner (Ref 5, 6) and also allows the refinement of intermetallics such as $CuAl_2$ and Mg_2Si particles, inducing chip breaking and optimization of the cutting operation of these materials (Ref 5). The production of small and brittle chips favors intermittent cutting, making chip extraction away from the cutting front easier, and inhibiting the formation of a builtup edge on the cutting edge of the tool. The formation of a builtup edge is usually associated to the machinability of alloys with low hardness and high ductility (Ref 7), production of long-continuous chips and high temperatures on the cutting front (Ref 8). Heating is favored by the high-cutting speeds, which are usually employed in machining aluminum alloys. Continuous and ductile chips are usually undesired and result in a poor surface finish.

Considering the facts mentioned above, three extruded-aluminum alloys, commonly used in the fabrication of hydraulic pumps, were studied. The alloy AA6106 with high and low P addition was tested on the recrystallized condition. The other two alloys, AA2117 and AA 6351, were tested in the cold-worked condition. The main difference between AA6351 and AA2117 is the 2.75 wt.% Cu addition in the AA2117. The specimens were chemically analyzed and had their tensile strength and hardness measured for their characterization, being tested, afterward in an instrumented drilling test in order to determine axial force and shear momentum. The aim was to correlate the metallurgical and mechanical characteristics to the machinability of the material in these conditions. For this work, the specimen that resulted in the lowest-drilling forces was considered best in terms of machinability.

2. Methodology

2.1 Metallurgical Characterization

The chemical composition of the studied alloys is shown in Table 1. One can observe that the AA 6061 alloys have different levels of Pb and Ti additions but are in the same recrystallized condition. The alloys AA2117 and AA6351 are on the cold-worked condition, and the AA2117 alloy has Cu addition, which is not present on the AA6351 alloy.

André R. Froehlich, Ricardo Callegari Jacques, Telmo R. Strohaecker, and **Ricardo Mombru,** Engineering, UFRGS, Oswaldo Aranha 99/610, Porto Alegre, Rio Grande do Sul 90035190, Brazil. Contact e-mail: rjacques@demet.ufrgs.br.

Table 1 Chemical analysis and microstructural condition of the aluminum alloys tested

Element (wt.%)	Alloy AA 6061 Low P	Alloy AA 6061 High P	Alloy AA 2117	Alloy AA 6351
Si	0.583	0.617	0.541	0.830
Fe	0.157	0.307	0.296	0.235
Cu	0.148	0.135	2.740	···
Mn	0.060	0.058	0.650	0.631
Mg	0.708	0.610	0.366	0.598
Cr	0.127	0.056	0.068	0.149
Zn	0.011	0.051	0.069	0.068
Pb	0.005	0.487	0.010	0.010
Ti	0.005	0.025	0.011	0.030
Microstructural Condition	Recrystallized	Recrystallized	Cold Worked	Cold Worked

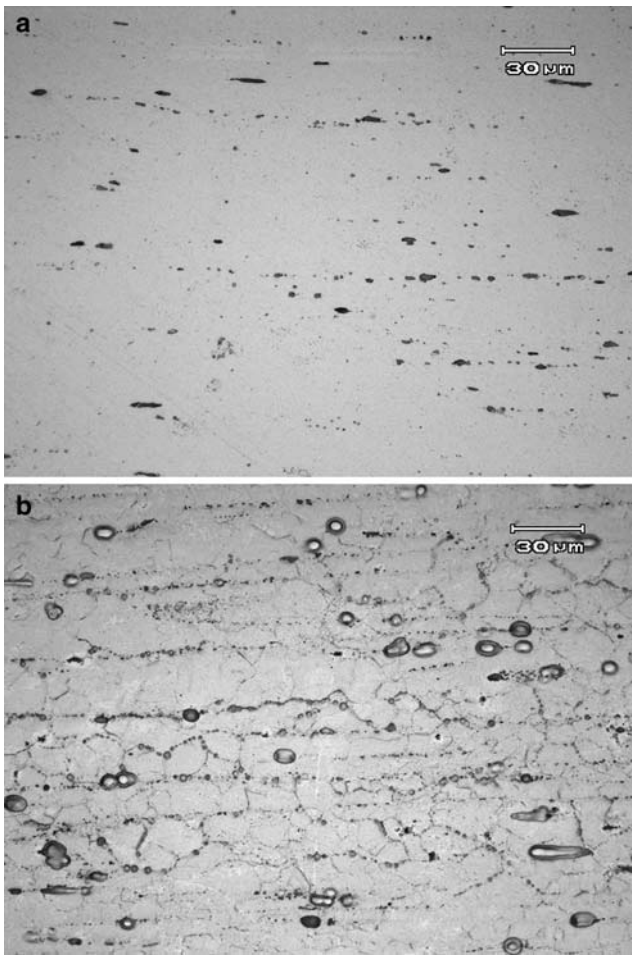

Fig. 1 Microstructure of the AA 6061 alloy without Pb additions. One can observe the lining up of magnesium-silicon particles (Mg_2Si). Etchants: (a) HF 0.5% and (b) Flick's

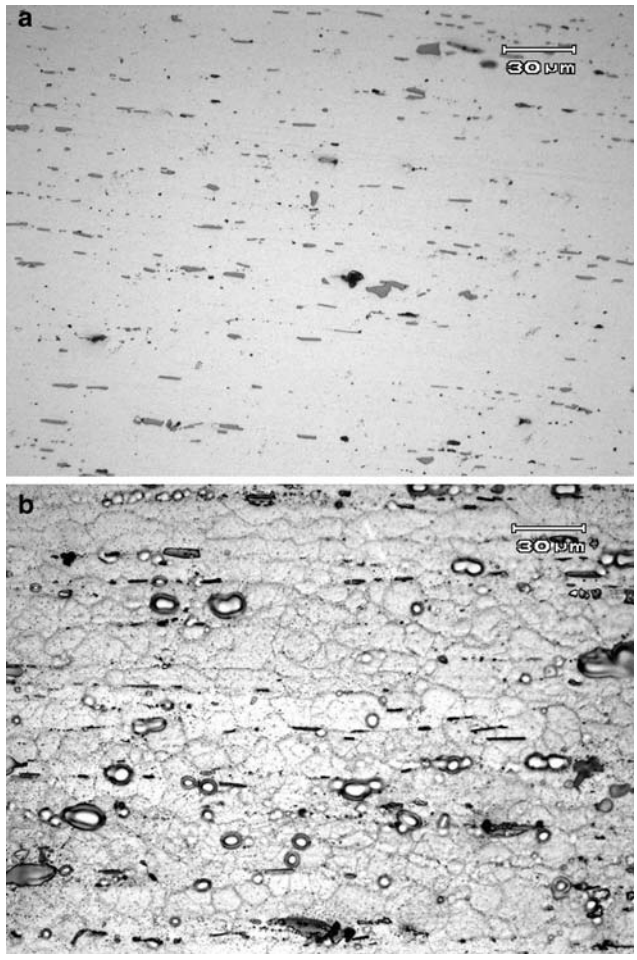

Fig. 2 Microstructure of AA 6061 alloy with Pb addition. Lining up of magnesium-silicon particles (Mg_2Si). Etchant: (a) HF 0.5% and (b) Flick's to reveal grain boundaries. Light micrograph

Figure 1, 2, 3, 4 show the microstructures of the studied alloys. Both samples of the AA6061 alloy are recrystallized, while the AA2117 and AA6351 alloys are in the cold-worked condition.

2.2 Tensile Strength and Hardness Tests

Samples with geometry according to E8M-98 (Fig. 9, specimen 5) standard were extracted for the tensile tests, which were made at room temperature. Samples were also produced for the hardness measurement on the Rockwell B scale.

2.3 Machining Forces Measurement

The samples were obtained from the extruded piece being identified, cut, and separated in two identical parts. The tests were done on both sides of the samples. Table 2 shows the characteristics of the drilling tool that was used. The drill was made of tool steel with a helical shape. The specific parameters used on the drilling are specified on Table 3.

The drilling time for each hole was around 2.9 s. The axial forces and shear momentum were measured with a piezoelectric load cell. Two specific signal conditioners are connected to the

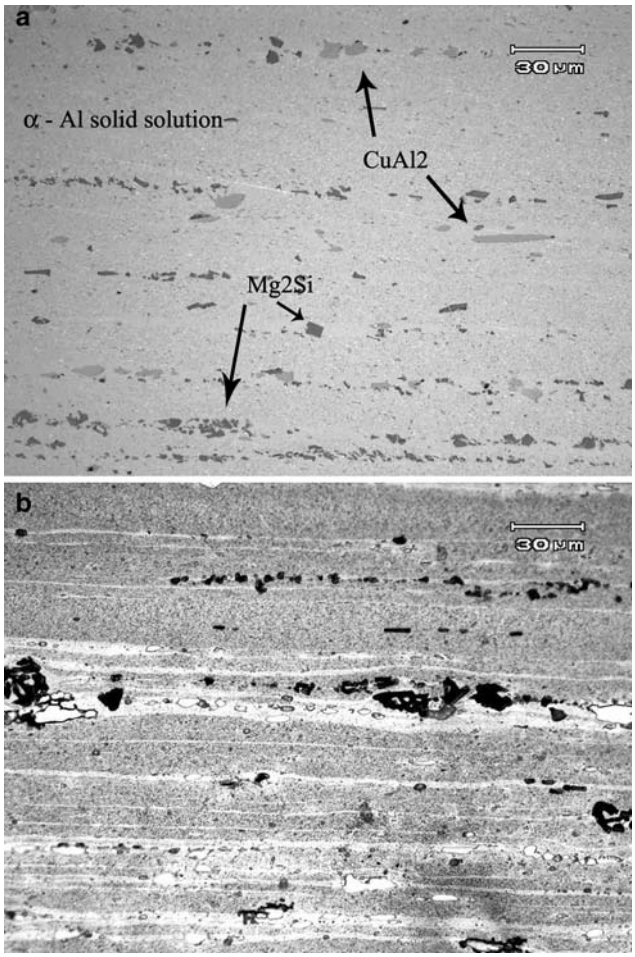

Fig. 3 Optical micrograph of AA 2117 alloy. One can see particles of $CuAl_2$ and Mg_2Si aligned with the extrusion direction. Etchant: (a) HF 0.5% and (b) H_2PO_4 10%

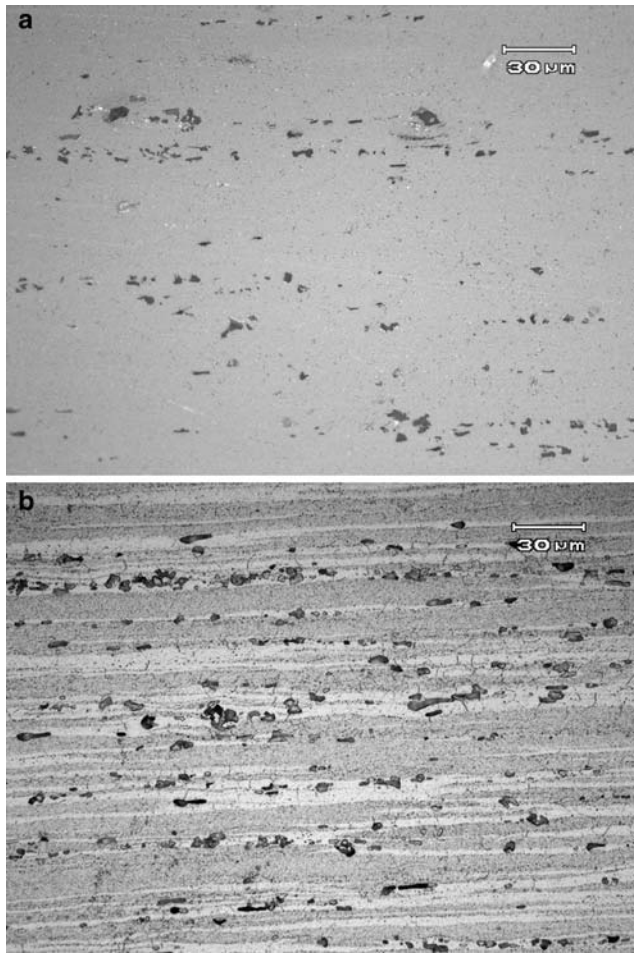

Fig. 4 Microstructure of AA 6351 alloy. One can see the lining up of magnesium-silicon particles (Mg_2Si). Etchant: (a) HF 0.5% and (b) H_2SO_4 10%. Light micrograph

Table 2 Characteristics of the tool used on the drilling tests

Type	Material	Standard	Name/Model	Dimensions, mm	Edge angle, σ	Helix Length, mm
Helical Drill	Tool Steel	DIN 333	IRWIN/HSS/10	∅10 × 133	118	87

Table 3 Machining parameters used for measurement of the drilling forces

Cutting Speed S_c (m/min)	Feeding rate of the tool f, mm/turn	Cutting length per hole, mm
80	0.2	25

cell and to a real time data acquisition system. Figure 5 shows the mounting of the machining tests.

3. Results

3.1 Tensile Test Results

Table 4 shows the tensile test results obtained for all specimens tested. The results presented are the averages of two tests for each sample.

3.2 Hardness Test Results

The results of the hardness tests for the different alloys are shown in Table 5. The results shown are the averaged value of five hardness measurements. The hardness for the AA6061 and AA6351 alloys are similar while the AA2117 alloy showed hardness higher than the others.

3.3 Microstructural Analysis

All alloys studied have shown a similar macrostructure, however, significant differences were observed in the microstructure. The alloys AA6061 (high and low Pb), showed similar microstructure: recrystallized α-aluminum with second phase particle aligned in the extrusion direction. As shown in Table 1, these alloys have lower Cu content when compared to alloy ASTM 2117 and because of this, there is only a minor occurrence of precipitates $CuAl_2$. In this alloy, the more frequent precipitates are rich in Mg, as the Mg_2Si precipitate.

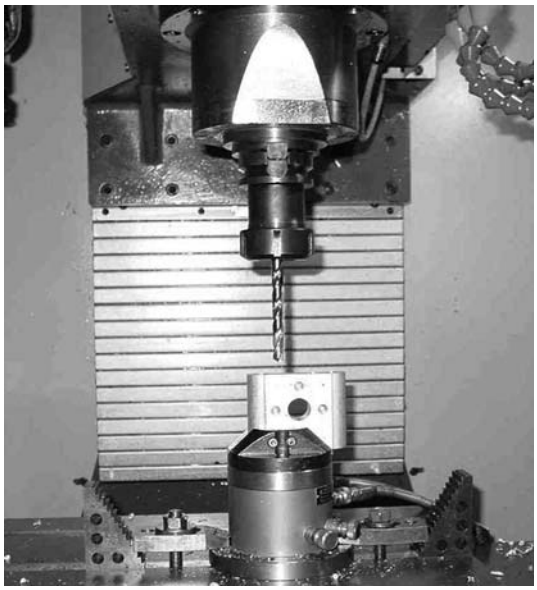

Fig. 5 Mounting of the system with the piezoelectric platform for the drilling tests

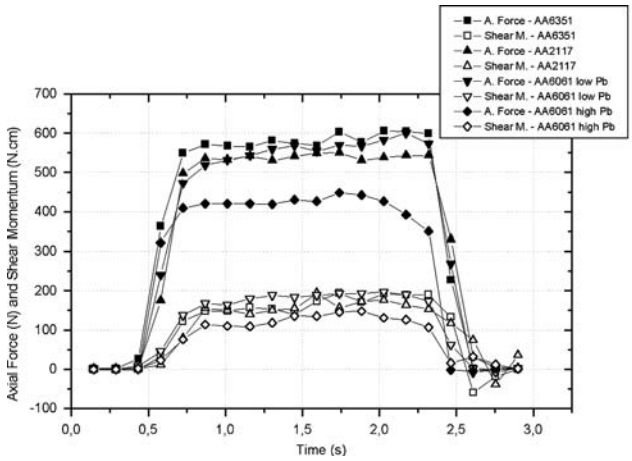

Fig. 6 Drilling Axial Force (N) and Shear Momentum (N cm) for the aluminum alloys studied

Table 4 Tensile test results for the aluminum alloys studied

	AA6061 Alloy Low Pb	AA6061 Alloy High Pb	AA 2117 Alloy	AA 6351 Alloy
$\sigma_{y,}$ MPa	310	308	272	263
UTS, MPa	342	338	423	441
Elongation, %	9.5	10.7	11.8	14.0

Table 5 Results of the hardness tests in HRB scale

AA6061 Alloy Low Pb	AA6061 Alloy High Pb	AA2117 Alloy	AA6351 Alloy
55.2	54.2	61.6	53

Table 6 Average values of axial force and shear momentum measured during drilling for the different alloys

	Alloy AA6061 low Pb	Alloy AA6061 high Pb	Alloy AA2117	Alloy AA6351
Axial Force (N)	560.4	425.9	539.4	580.2
Shear Momentum (N cm)	183.4	125.5	160.5	164.9

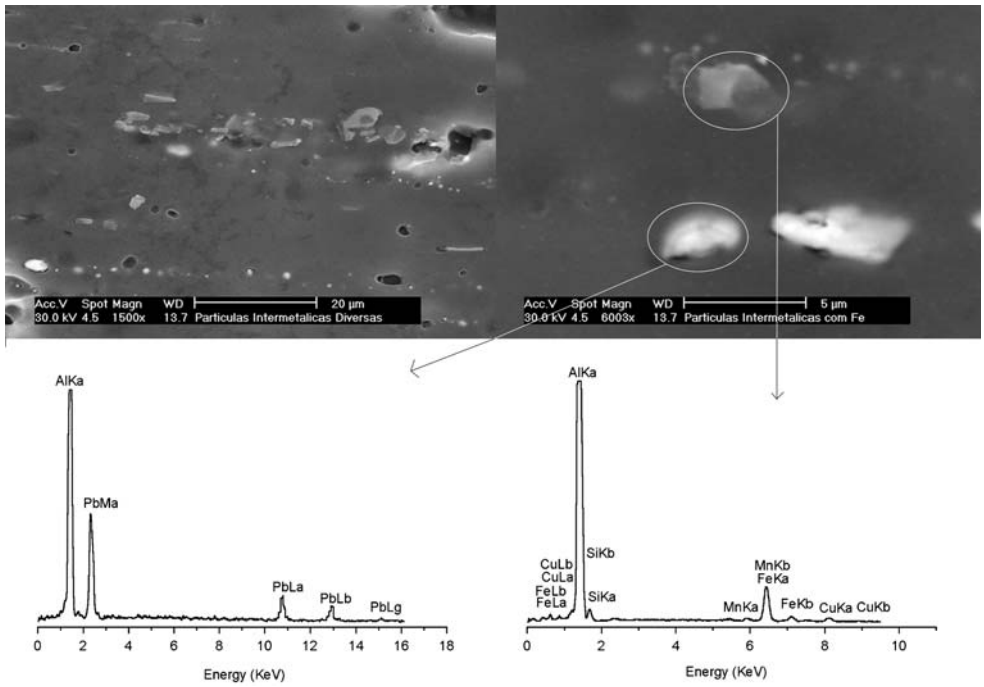

Fig. 7 SEM and EDX analysis of high Pb AA 6061 alloy and intermetallics rich in Fe, Mn and Cu

The hardness values for the AA6061 and AA6351 alloys are similar and lower than those observed on the AA2117 alloy.

The microstructure of the AA2117 alloy shows $CuAl_2$ and Mg_2Si precipitates aligned to the extrusion direction. This characteristic is also observed on the AA6351 alloy, whose microstructure is shown in Fig. 3. The values of hardness of these two alloys, shown in Table 5, indicate that the alloy AA2117 has higher hardness than the alloy AA6351. This is due to the Cu addition, which increases hardness and mechanical resistance in aluminum alloys.

3.4 Axial Force (N) and Shear Momentum (N cm)

Figure 6 shows the axial force and shear momentum as a function of time for each of the tested materials. Each curve represents the mean value of seven drilling operations for each alloy.

Table 6 shows the average shear momentum and axial forces measured during the drilling of the extruded bars.

The high Pb AA6061 alloy showed a significant lower-axial force than the other alloys. A reduction of 21% in the axial force was achieved when comparing the high P AA6061 with the AA2117 alloy, which showed the second lowest-axial force.

4. Discussion

Considering the metallurgical characteristics of the extruded aluminum alloys that were studied and analyzed and the great amount of bibliographic data regarding the effects of these properties on the machinability of these alloys, the information found in the literature was confronted with the actual results found in the tests.

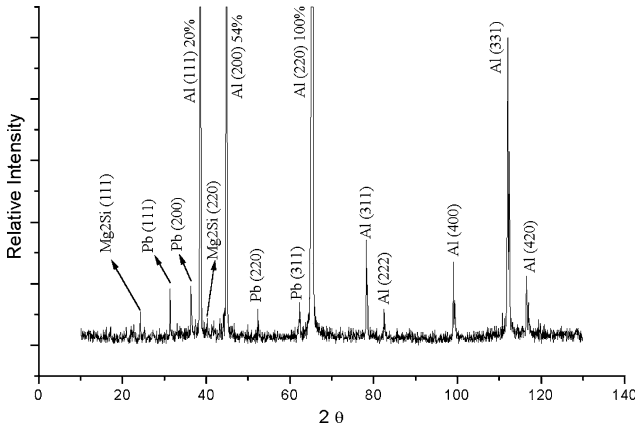

Fig. 8 X-Ray diffraction of high P AA 6061 alloy

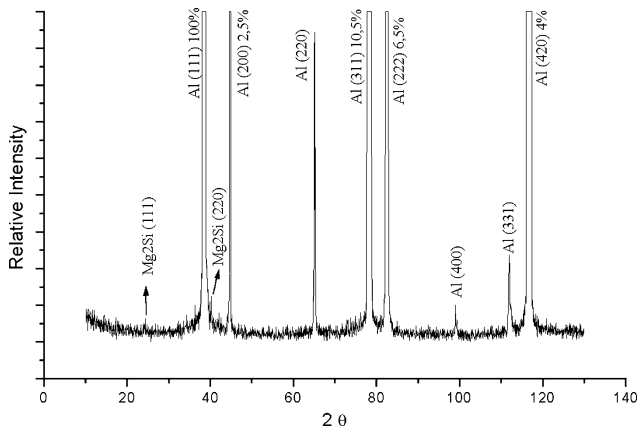

Fig. 10 X-Ray diffraction of the low P AA6061 alloy

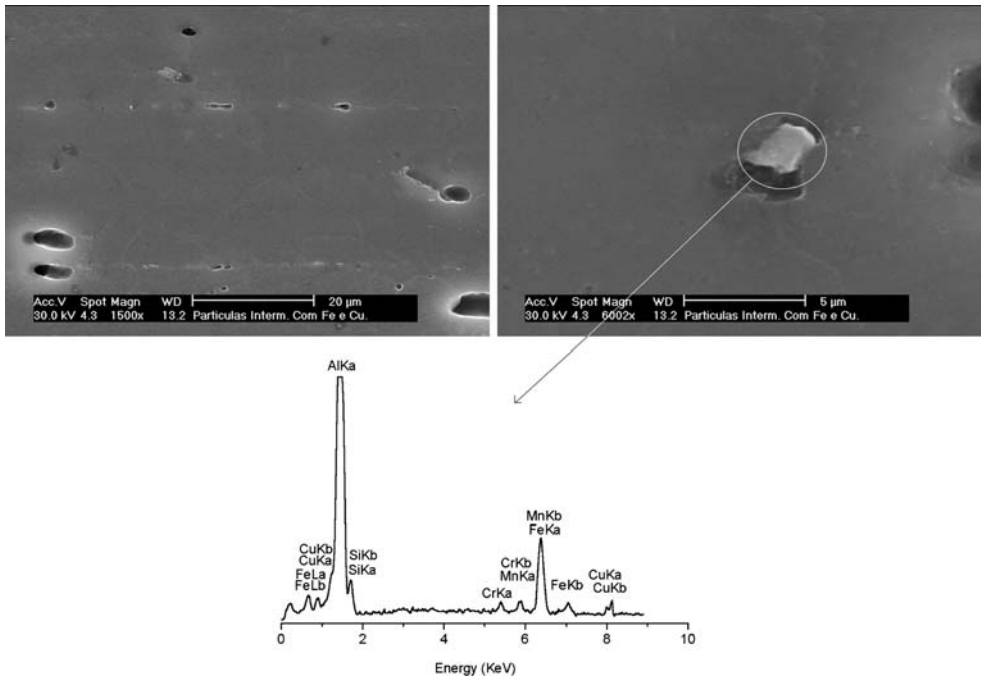

Fig. 9 Scanning electron micrograph and EDS spectrum for a selected precipitate present in the low Pb AA6061 alloy

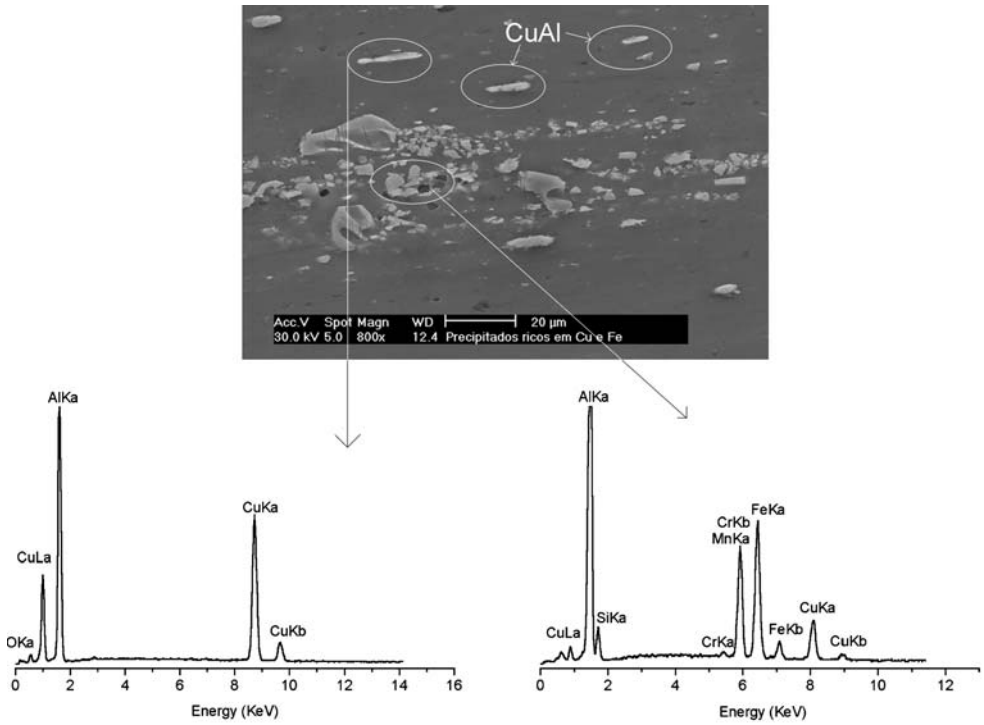

Fig. 11 SEM and EDS of the AA 2117 alloy. One can see the presence of intermetallics rich in Fe, Mn, Cr and Cu

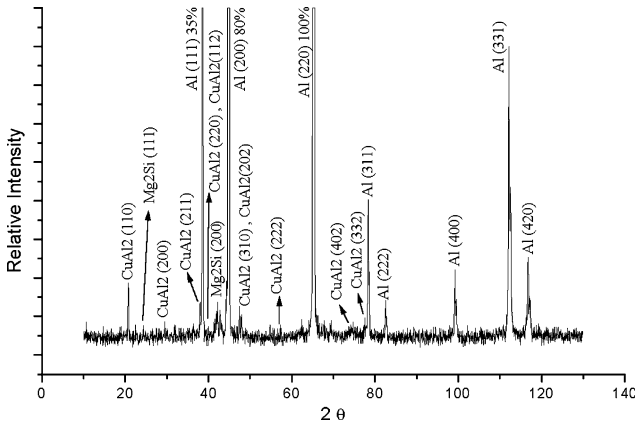

Fig. 12 X-Ray Diffraction pattern of the alloy AA2117 with the presence of $CuAl_2$

For AA 6061 alloys, the presence of Pb in amounts of 0.49% would have a positive effect in machinability compared to the same alloys without this element, for Pb acts as a chip breaker (Ref 1, 2) and as tool lubricant. The measuring of the cutting forces indeed indicated that the lowest-machining forces occurred on this alloy with the presence of Pb. Both the scanning electron microscope with EDX and the x-ray diffraction revealed the presence of this element in the form of disperse particles in the microstructural matrix, as can be seen in Fig. 7 and 8. Besides, this alloy has amounts of Ti that favor microstructural refinement and induce precipitate dispersion in general, contributing for the production of small and brittle chips.

Besides the presence of Pb particles, intermetallics rich in Fe and Mn were also found to be dispersed finely in the matrix. These precipitates stimulate the production of small and loose chips, which are better for machining.

Figure 8 shows the x-ray results confirming the presence of Pb on the AA6061 alloy, which had the lowest-machining forces. The presence of intermetallic Mg_2Si is also observed, which, according to the literature, confers good machinability characteristics to aluminum alloys.

The low Pb AA6061 alloy showed machining forces significantly higher than the same alloy with high Pb. The axial force was 560.4 N compared to the 425.9 N measured in the alloy with Pb additions, while the shear momentum was 183.4 N cm compared to 125.5 N cm in the alloy with Pb additions.

Figure 9 shows the scanning electron microscope and EDS analysis of the low Pb AA6061 alloy. No Pb particles were observed on this alloy. Detailed analysis of the precipitates indicate only the presence of disperse intermetallics rich in Fe, Cr, Mn, and Cu. The amounts of Si and Mg on this alloy, as shown in Table 1, indicate that Mg_2Si intermetallics should be present, with beneficial effects on the machinability of the material. Figure 10 shows the x-ray diffraction pattern for this alloy. One can see a minor occurrence of Mg_2Si intermetallic. In spite of the presence of Fe, Mn Cr, Cu and Mg_2Si intermetallics, the effect upon the machinability forces was not as significant as the effect of Pb on the alloy AA6061.

It should be noticed that both the tensile strength and hardness of these two alloys were similar and the better/worse machinability of one of the alloys cannot be thus justified. The lesser-machinability forces are associated to the metallurgical properties related to the presence of Pb on the alloy. It should also be noticed that this alloy had the best behavior of all four studied alloys.

Figure 11 shows EDS and microstructural analysis of the alloy AA2117, which significantly has a higher amount of Cu compared to the other alloys. Copper is reported in literature as a former of $CuAl_2$, which acts as a chip breaker when finely

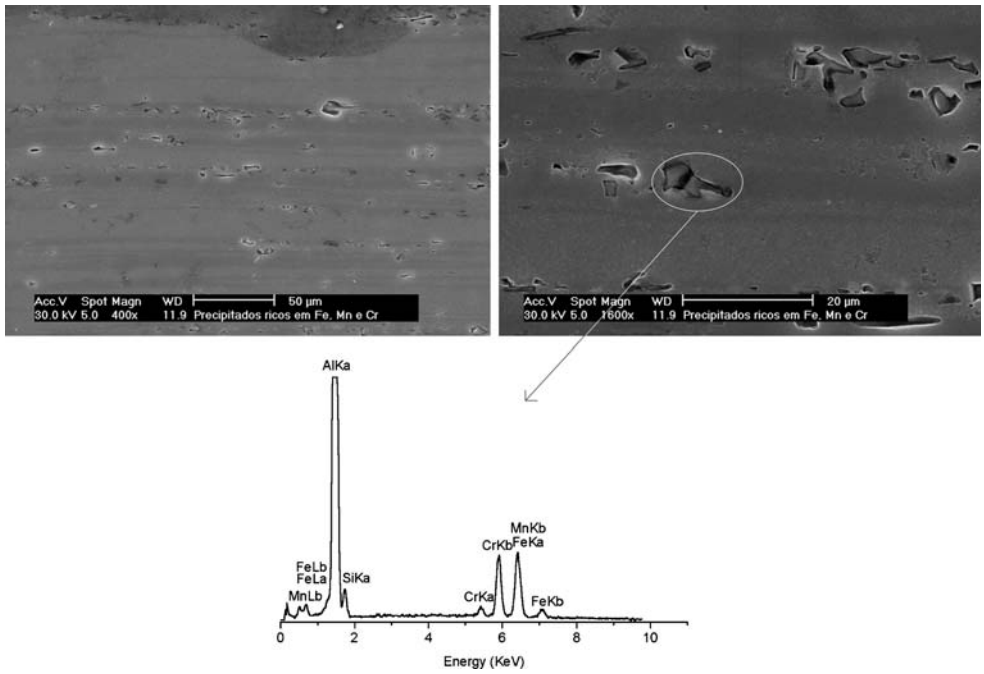

Fig. 13 SEM and EDS of AA 6351 alloy. One can see the presence of intermetallics rich in Fe, Mn, Cr and Cu

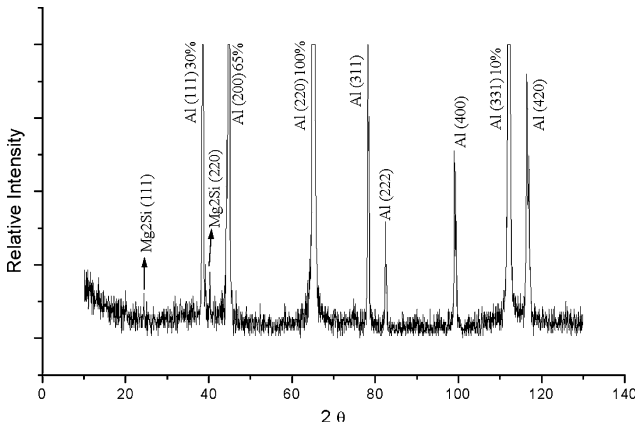

Fig. 14 X-Ray diffraction pattern of the AA6351 alloy indicating the presence of Mg_2Si precipitates

disperse in the matrix. Even though it has a higher hardness than the AA6061 alloys and it is cold worked, the AA 2117 alloy showed a better machinability than the low Pb AA 6061 alloy with axial force of 539.4 N and shear momentum of 160.5 N cm. Both these values were the second lowest-machining efforts that were measured. This behavior is associated to the presence of $CuAl_2$ precipitates and finely disperses intermetallics rich in Fe, Mn and Cr. Figure 12 presents the x-ray diffraction pattern of this alloy, showing the presence of $CuAl_2$ and Mg_2Si. However, the results show that their presence has a lesser influence when comparing to the influence of the presence of Pb.

Alloy AA6351, which does not have Cu additions as in the alloy AA2117, was the material which had the highest-axial force, 580.1 N, and shear momentum, 164.9 N cm. Figure 13 shows the microstructural analysis and the EDX, characterizing the absence of intermetallic precipitates of the type $CuAl_2$. The EDX analysis clearly shows the presence of intermetallic precipitates rich in Fe, Mn and Cr as expected for this alloy.

Although the metallographic characterization of this alloy did not indicate the presence of Mg_2Si precipitates, their presence was detected by the x-ray analysis, as shown in Fig. 14. The only second phase present in this alloy was Mg_2Si.

In the view of the mechanical properties, this alloy had hardness similar to those presented by both low and high P AA6061. However, the AA6351 alloy had the highest-axial force in the drilling tests of all the alloys studied. This behavior is associated to the absence of elements and metallurgical aspects that favor chip embrittlement such as the presence of Pb particles and intermetallics of the type $CuAl_2$. The only particles observed were small quantities Mg_2Si.

5. Conclusions

The current work shows the influence of metallurgical aspects such as chemical composition and the presence of microstructural precipitates upon the machinability of the studied aluminum alloys.

The analysis in the metallurgical aspect indicate that the alloy AA 6061 with Pb and Ti additions would have a better machinability compared to the other analyzed alloys, which is confirmed with the results obtained from the drilling tests. The beneficial effects of the presence of Pb and Ti in the optimization of the aspects related to the decreasing of energies and costs for the machinability of these alloys were indeed confirmed.

The beneficial effects of the $CuAl_2$ precipitates upon machinability are also reported in the literature and confirmed on the current work, where we conclude that the alloy AA 2117, even cold worked and with a higher hardness compared to the others, has the second lowest-axial forces and shear momentum measured. Apparently, the cold-worked condition

associated to the presence of $CuAl_2$ has a tendency of favoring the embrittlement of the chips and resulting in a lower tendency of adhesion of the alloy upon the cutting edge, thus improving alloy machinability.

The results also indicate the beneficial effects of the different precipitates upon the machinability of the studied alloys may be cited in a decreasing order of importance as: presence of Pb precipitates finely disperse in the matrix (favored by the presence of Ti), presence of $CuAl_2$ precipitates in the same conditions and, at last, the presence of Mg_2Si precipitates. It should be remarked, though, that the Mg_2Si precipitates have only a minor presence in the studied alloys.

This work confirms the influence of metallurgical factors upon the machinability of the extruded aluminum alloys. Thus, we conclude that the efforts in the search of production gain with cost reduction, decrease in tool wear, energy costs, and machining times must consider, besides the mechanical aspects such as speed and cutting feeds, lubricants and tool design, and the microstructure of the material, which is to be machined, in a way to favor lesser cutting forces and optimization of the production procedures.

References

1. V.O. Abramov, O.V. Abramov, F. Sommer, and D. Orlov, Influence of Si Addition on the Microstructure and the Properties of Al-Pb Base Alloys Prepared Under Quasi-weightlessness Condition, *Materials Letters*, 1996, **29**, p 67–71
2. ASM Handbook, "Properties and Selection: Nonferrous Alloys and Special-Purpose Materials," *Metals Handbook Vol. 2* 10th Ed
3. ASM, *Aluminum – Properties and Physical Metallurgy*, Constitution of Alloys Chapter 2 and Properties of Commercial Casting Alloys, 1984, Chap. 8
4. J.D. Edwards, F.C. Frary, and Z. Jeffries, *The Aluminum Industry – Aluminum Products and Their Fabrication*, Chapter IV – Properties of Aluminum alloys, p. 176
5. W.L. Weingaertner and R.B. Schroeter, Tecnologia de Usinagem do Alumínio e suas Ligas (Machining Technology of Aluminum and its alloys) – Usinagem do Alumínio (Machining of Aluminum), Chap. 6, p. 42, (in Portuguese)
6. *Aluminum Permanent Mold Handbook* – AFS, 2001, Chap. 1, p. 7
7. Dieter, G.E. *Mechanical Metallurgy*, Machining of Metals, Chap. 21 p. 689
8. M. Nouari, G. List, F. Girot, and D. Coupard, Experimental Analysis and Optimisation of Tool Wear in Dry Machining of Aluminium Alloys, *Wear*, 2003, **255**, p 1359–1268